Large-basis shell-model calculations for *p*-shell nuclei

P. Navrátil* and B. R. Barrett
Department of Physics, University of Arizona, Tucson, Arizona 85721
(Received 19 February 1998)

Results of large-basis shell-model calculations for nuclei with $A=7-11$ are presented. The effective interactions used in the study were derived microscopically from the Reid93 potential and take into account the Coulomb potential as well as the charge dependence of $T=1$ partial waves. For $A=7$, a $6\hbar\Omega$ model space was used, while for the rest of the studied nuclides, the calculations were performed in a $4\hbar\Omega$ model space. It is demonstrated that the shell model combined with microscopic effective interactions derived from modern nucleon-nucleon potentials is capable of providing good agreement with the experimental properties of the ground state as well as with those of the low-lying excited states. [S0556-2813(98)07806-6]

PACS number(s): 21.60.Cs, 21.10.Dr, 21.10.Ky, 27.20.+n

I. INTRODUCTION

Large-basis no-core shell-model calculations have recently been performed [1–11]. In these calculations all nucleons are active, which simplifies the effective interaction as no hole states are present. In the approach taken, the effective interaction derived microscopically from modern nucleon-nucleon potentials is determined for a system of two nucleons only and subsequently used in the many-particle calculations. To take into account a part of the many-body effects, a so-called multivalued effective interaction approach was introduced and applied in the no-core shell-model calculations [8].

In the past, these calculations concentrated on the $0s$-shell nuclei and $A=5,6$ $0p$-shell nuclei. In addition, ^{7}Li was studied in a $4\hbar\Omega$ model-space calculation [8] and the obtained wave-functions were employed for evaluating proton and electron scattering characteristics [12]. Large-basis no-core shell-model calculations for heavier $0p$-shell nuclei have not been discussed until recently. In the most recent application, we applied the no-core shell-model approach to the $A=10$ nuclei in order to evaluate the isospin-mixing correction to the Fermi matrix element $^{10}\mathrm{C}\rightarrow{}^{10}\mathrm{B}$ [11]. In the present paper we complement this study by presenting the results for other light $0p$-shell nuclides. In particular, we present calculations for the $A=7$ nuclei ^{7}He, ^{7}Li, ^{7}Be, and ^{7}B performed in a $6\hbar\Omega$ model space, in which configurations up to an energy of $6\hbar\Omega$ relative to the unperturbed ground-state configuration are included. For $A=8$, results were obtained for ^{8}He, ^{8}Li, ^{8}Be, and ^{8}B in a $4\hbar\Omega$ model space. For $A=9$ we calculated properties of ^{9}He, ^{9}Li, ^{9}Be, ^{9}B, and ^{9}C also in a $4\hbar\Omega$ model space. As the $A=10$ nuclides ^{10}C, ^{10}B, and partly ^{10}Be, were discussed in Ref. [11], we now complete the $A=10$ nuclei description by including results for ^{10}He, ^{10}Li, and ^{10}Be. Finally, we give the results of a $4\hbar\Omega$ calculation for ^{11}Li and ^{11}Be.

Our study is distinguished from other $0p$-shell-nuclei calculations by the fact that we are using microscopically derived effective interactions, contrary to phenomenological interactions employed in most other papers [13–17]. The other distinguishing factor is the use of large multiconfiguration model spaces.

The organization for the paper is as follows. First, in Sec. II we discuss the shell-model Hamiltonian with a bound center-of-mass and the method used to derive the starting-energy-independent effective interaction. Results of the calculations for $A=7-11$ are presented in Sec. III and concluding remarks are given in Sec. IV.

II. THE SHELL-MODEL HAMILTONIAN AND EFFECTIVE INTERACTION

In the present paper we apply the approach discussed in Refs. [9,11]. We start with the one- plus two-body Hamiltonian for the A-nucleon system, i.e.,

$$H^{\Omega}=\sum_{i=1}^{A}\frac{\vec{p}_i^{\,2}}{2m}+\sum_{i<j}^{A}V_{\mathrm{N}}(\vec{r}_i-\vec{r}_j)+\frac{1}{2}Am\Omega^2\vec{R}^2, \qquad (1)$$

where m is the nucleon mass, $V_{\mathrm{N}}(\vec{r}_i-\vec{r}_j)$ the nucleon-nucleon interaction, and $\frac{1}{2}Am\Omega^2\vec{R}^2$ [$\vec{R}=(1/A)\Sigma_{i=1}^{A}\vec{r}_i$] is the center-of-mass harmonic-oscillator potential. The latter potential does not influence intrinsic properties of the many-body system. It provides, however, a mean field felt by each nucleon and allows us to work with a convenient harmonic-oscillator basis. The Hamiltonian (1), depending on the harmonic-oscillator frequency Ω, may be cast into the form

$$H^{\Omega}=\sum_{i=1}^{A}\left[\frac{\vec{p}_i^{\,2}}{2m}+\frac{1}{2}m\Omega^2\vec{r}_i^{\,2}\right]+\sum_{i<j}^{A}\left[V_{\mathrm{N}}(\vec{r}_i-\vec{r}_j)-\frac{m\Omega^2}{2A}(\vec{r}_i-\vec{r}_j)^2\right]. \qquad (2)$$

The one-body term of the Hamiltonian (2) is then rewritten as a sum of the center-of-mass term $H^{\Omega}_{\mathrm{cm}}=\vec{P}^{\,2}_{\mathrm{cm}}/2Am+\frac{1}{2}Am\Omega^2\vec{R}^2$, $\vec{P}_{\mathrm{cm}}=\Sigma_{i=1}^{A}\vec{p}_i$, and a term depending only on relative coordinates. Shell-model calculations are carried out in a model space defined by a projector P. In the present

*On leave of absence from the Institute of Nuclear Physics, Academy of Sciences of the Czech Republic, 250 68 Řež near Prague, Czech Republic.

work, we will always use a complete $N\hbar\Omega$ model space which includes all the configurations up to an energy of $N\hbar\Omega$ relative to the unperturbed ground-state configuration. The complementary space to the model space is defined by the projector $Q=1-P$. In addition, from among the eigenstates of the Hamiltonian (2), it is necessary to choose only those corresponding to the same center-of-mass energy. This can be achieved by projecting the center-of-mass eigenstates with energies greater than $\frac{3}{2}\hbar\Omega$ upwards in the energy spectrum. The shell-model Hamiltonian, used in the actual calculations, takes the form

$$H_{P\beta}^{\Omega}=\sum_{i<j=1}^{A} P\left[\frac{(\vec{p}_i-\vec{p}_j)^2}{2Am}+\frac{m\Omega^2}{2A}(\vec{r}_i-\vec{r}_j)^2\right]P + \sum_{i<j}^{A} P\left[V_{\mathrm{N}}(\vec{r}_i-\vec{r}_j)-\frac{m\Omega^2}{2A}(\vec{r}_i-\vec{r}_j)^2\right]_{\mathrm{eff}}P + \beta P\left(H_{\mathrm{cm}}^{\Omega}-\frac{3}{2}\hbar\Omega\right)P, \tag{3}$$

where β is a sufficiently large positive parameter. In Eq. (3), the notation $[\ ]_{\mathrm{eff}}$ means that the quantity within the square brackets is the residual interaction to be used in the determination of the effective interaction within the model space P (see Ref. [9] for more details).

The effective interaction introduced in Eq. (3) should, in principle, exactly reproduce the full-space results in the model space for some subset of states. In practice, the effective interactions can never be calculated exactly, because, in general, for an A-nucleon system an A-body effective interaction is required. Consequently, large model spaces are desirable when only an approximate effective interaction is used. In that case, the calculation should be less affected by any imprecision of the effective interaction. The same is true for the evaluation of any observable characterized by an operator. In the model space, renormalized effective operators are also required. The larger the model space, the less renormalization is needed.

Usually, the effective interaction is approximated by a two-body effective interaction determined from a two-nucleon system. In this study, we use the procedure, as described in Ref. [9]. To construct the effective interaction we employ the Lee-Suzuki [18] similarity transformation method, which gives an interaction in the form $P_2V_{\mathrm{eff}}P_2=P_2VP_2+P_2VQ_2\omega P_2$, with ω the transformation operator satisfying $\omega=Q_2\omega P_2$. The projection operators $P_2, Q_2=1-P_2$ project on the two-nucleon model and complementary spaces, respectively. Note that we distinguish the two-nucleon system projection operators P_2, Q_2 from the A-nucleon system operators P, Q. Our calculations start with exact solutions of the Hamiltonian

$$H_2^{\Omega}\equiv H_{02}^{\Omega}+V_2^{\Omega}=\frac{\vec{p}_1^{\,2}+\vec{p}_2^{\,2}}{2m}+\frac{1}{2}m\Omega^2(\vec{r}_1^{\,2}+\vec{r}_2^{\,2}) + V_N(\vec{r}_1-\vec{r}_2)-\frac{m\Omega^2}{2A}(\vec{r}_1-\vec{r}_2)^2, \tag{4}$$

which is the shell-model Hamiltonian (2) applied to a two-nucleon system. We construct the effective interaction directly from these solutions. Let us denote the two-nucleon harmonic-oscillator states, which form the model space, as $|\alpha_P\rangle$, and those which belong to the Q-space as $|\alpha_Q\rangle$. Then the Q-space components of an eigenvector $|k\rangle$ of the Hamiltonian (4) can be expressed as a combination of the P-space components with the help of the operator ω,

$$\langle\alpha_Q|k\rangle=\sum_{\alpha_P}\langle\alpha_Q|\omega|\alpha_P\rangle\langle\alpha_P|k\rangle. \tag{5}$$

If the dimension of the model space is d_P, we may choose a set $\mathcal{K}$ of d_P eigenvectors, typically the lowest states obtained in each channel, for which the relation (5) will be satisfied. Under the condition that the $d_P\times d_P$ matrix $\langle\alpha_P|k\rangle$ for $|k\rangle\in\mathcal{K}$ is invertible, the operator ω can be determined from Eq. (5). Once the operator ω is determined, the effective Hamiltonian can be constructed as follows:

$$\langle\gamma_P|H_{2\mathrm{eff}}|\alpha_P\rangle=\sum_{k\in\mathcal{K}}\left[\langle\gamma_P|k\rangle E_k\langle k|\alpha_P\rangle+\sum_{\alpha_Q}\langle\gamma_P|k\rangle E_k\langle k|\alpha_Q\rangle\langle\alpha_Q|\omega|\alpha_P\rangle\right]. \tag{6}$$

This Hamiltonian, when diagonalized in a model-space basis, reproduces exactly the set $\mathcal{K}$ of d_P eigenvalues E_k. Note that the effective Hamiltonian is, in general, quasi-Hermitian. It can be hermitized by a similarity transformation determined from the metric operator $P_2(1+\omega^{\dagger}\omega)P_2$. The Hermitian Hamiltonian is then given by [19]

$$\overline{H}_{2\mathrm{eff}}=[P_2(1+\omega^{\dagger}\omega)P_2]^{1/2}H_{2\mathrm{eff}}[P_2(1+\omega^{\dagger}\omega)P_2]^{-1/2}. \tag{7}$$

Finally, the two-body effective interaction used in the present calculations is determined from the two-nucleon effective Hamiltonian (7) as $V_{\mathrm{eff}}=\overline{H}_{2\mathrm{eff}}-H_{02}^{\Omega}$.

To at least partially take into account the many-body effects neglected when using only a two-body effective interaction, we employ the recently introduced, so-called, multivalued effective interaction approach [8]. In that approach, different effective interactions are used for different harmonic-oscillator excitations of the spectators. The effective interactions then carry an additional index indicating the sum of the oscillator quanta for the spectators, N_{sps}, defined by

$$N_{\mathrm{sps}}=N_{\mathrm{sum}}-N_{\alpha}-N_{\mathrm{spsmin}}=N'_{\mathrm{sum}}-N_{\gamma}-N_{\mathrm{spsmin}}, \tag{8}$$

where N_{sum} and N'_{sum} are the total oscillator quanta in the

initial and final many-body states, respectively, and N_α and N_γ are the total oscillator quanta in the initial and final two-nucleon states $|\alpha\rangle$ and $|\gamma\rangle$, respectively. $N_{\rm spsmin}$ is the minimal value of the spectator harmonic-oscillator quanta for a given system. For example, for $A=7$, $N_{\rm spsmin}=1$. Different sets of the effective interaction are determined for different model spaces characterized by $N_{\rm sps}$ and defined by projection operators

$$Q_2(N_{\rm sps})=\begin{cases}0 & \text{if } N_1+N_2\leq N_{\rm max}-N_{\rm sps},\\ 1 & \text{otherwise;}\end{cases} \tag{9a}$$

$$P_2(N_{\rm sps})=1-Q_2(N_{\rm sps}). \tag{9b}$$

In Eqs. (9), $N_{\rm max}$ characterizes the two-nucleon model space. It is an input parameter chosen in relation to the size of the many-nucleon model space. This multivalued effective-interaction approach is superior to the traditional effective interaction, as confirmed also in a model calculation [20].

III. APPLICATION TO THE *P*-SHELL NUCLEI

We apply the formalism outlined in Sec. II for selected $0p$-shell nuclei. In the calculations we use the Reid93 nucleon-nucleon potential [21] and consider the following isospin-breaking contributions. First, the Reid93 potential differs in the $T=1$ channels for proton-neutron (pn) and proton-proton (pp), neutron-neutron (nn) systems, respectively. Second, we add the Coulomb potential to the pp Reid93 potential. Consequently, using Eqs. (5)–(7), we derive different two-body effective interactions for the pn, pp, and nn systems.

As we derive the effective interaction microscopically from the nucleon-nucleon interaction, the number of freely adjustable parameters in the calculation is limited. First, we have the choice of the model-space size in the shell-model diagonalization. That is, however, constrained by computer capabilities. The largest model space we were able to use was the space allowing all $6\hbar\Omega$ excitations relative to the unperturbed ground state for $A=7$ nuclei and all $4\hbar\Omega$ excitations relative to the unperturbed ground state for $A>7$ nuclei, respectively. The calculations were done in the m-scheme using the many-fermion-dynamics code [22] extended to allow the use of different pn, pp, and nn interactions. We note that in this study the same effective interaction is used for each isobaric chain, and thus the same model-space size is employed for all the isobars of given A.

Second, our effective interactions depend on the choice of the two-nucleon model space size. The two-nucleon model space size is related to the many-nucleon model-space size, and, in principle, is determined by that size. Traditionally, however, the $Q_2=0$ space used to determine the G-matrix does not, necessarily, coincide with the many-particle model space [23,24]. In our calculation, the two-nucleon model space is characterized by a restriction on the number of harmonic-oscillator quanta $N_1\leq N_{\rm max}$, $N_2\leq N_{\rm max}$, $(N_1+N_2)\leq N_{\rm max}$. Here, $N_i=2n_i+l_i$ is the harmonic-oscillator quantum number for the nucleon $i, i=1,2$. This type of restriction guarantees an orthogonal transformation between the two-particle states and the relative- and center-of-mass-coordinate states. With regard to the $4\hbar\Omega$ calculation for the $0p$-shell nuclei, the choice of $N_{\rm max}=6$ appears to be appropriate. However, it has been observed in the past [4,7,9] that when the Lee-Suzuki procedure is combined with the G-matrix calculation according to Ref. [23] (which is equivalent to the procedure we are using) and is applied to calculate the two-body effective interaction, the resulting interaction may be too strong. This is, in particular, true, when the multivalued approach is used. The reason for this is likely the fact that our effective interaction is computed for a two-nucleon system bound in a harmonic-oscillator potential. Therefore, artificial binding from this potential is included in the effective interaction and the many-body effects coming from the large-basis space calculation do not completely compensate for this spurious binding. This effect decreases when the model-space size increases as is demonstrated in our earlier three-nucleon shell-model calculations [25]. Several possible adjustments have been discussed to deal with this problem [4,9] in smaller model spaces and amount to introducing an extra parameter. In the present calculations, we use two methods introduced in the previous papers. For the $A=10$ $4\hbar\Omega$ calculation presented in Ref. [11], we preferred to treat $N_{\rm max}$ as a free parameter and use $N_{\rm max}=8$ for the $4\hbar\Omega$ calculations. With this choice, which results in an overall weaker interaction than that calculated with $N_{\rm max}=6$, we obtain quite reasonable binding energies for all the studied nuclei. This approach is employed here for the $4\hbar\Omega$ calculations for the nuclei with $A>7$. On the other hand, in the case of $A=7$ for the $6\hbar\Omega$ space we follow Ref. [9] and use the parameter k_Q introduced there. While for $k_Q=1$ there is no modification, the choice of $k_Q<1$ reduces the contribution of the Q_2-space part of the harmonic-oscillator potential on the two-nucleon effective interaction. For this calculation, $N_{\rm max}=8$ appropriate for the $6\hbar\Omega$ many-nucleon space size is employed. In Ref. [9] we used this approach for the $6\hbar\Omega$ calculations for $A=5$ and 6 nuclei as well as for the $8\hbar\Omega$ calculations for $A=3$ and 4 nuclei. We note that we are studying ways in which to eliminate these extra parameters by means of renormalizations of the two-body effective interactions utilizing knowledge of the three-body effective interactions. The three-body effective interactions can be calculated following the approach introduced in Ref. [25].

Finally, our results depend on the harmonic-oscillator frequency Ω. We have studied this dependence by performing calculations for the values $\hbar\Omega=14$, 15.5, and 17 MeV for ^{10}C and ^{10}B in Ref. [11]. Here we present the same dependence for ^{10}Li. For the other studied nuclei we choose $\hbar\Omega$ in the range 15–17 MeV. We keep the same value of $\hbar\Omega$ for each isobaric chain.

Let us note that our calculations do not violate the separation of the center-of-mass and the internal relative motion. In particular, a variation of the parameter β introduced in Eq. (3) does not change the eigenenergies and other characteristics of the physical states. This is so due to the utilization of a complete $N\hbar\Omega$ many-nucleon model space and the triangular two-nucleon model space for deriving the effective interaction as well as due to the procedure used to derive the effective interaction.

A. $A=7$ nuclei

In Figs. 1, 2, 3, and 4 we present the experimental and calculated excitation spectra of ^{7}He, ^{7}Li, ^{7}Be, and ^{7}B, re-

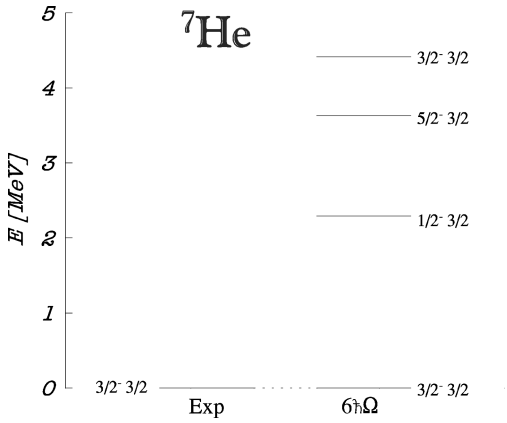

FIG. 1. The experimental and calculated excitation spectra of ^{7}He. The results corresponding to the model-space size of $6\hbar\Omega$ relative to the unperturbed ground-state configuration are presented. A harmonic-oscillator energy of $\hbar\Omega = 17$ MeV was used.

spectively. Their ground-state properties are summarized in the first part of Table I. The calculations were performed in the $6\hbar\Omega$ model space. A harmonic-oscillator frequency of $\hbar\Omega = 17$ MeV was used. As discussed earlier in this section, we employed the additional parameter k_Q, introduced in Ref. [9], and set its value to $k_Q = 0.8$. Note that for ^{7}Li and ^{7}Be, the dimension in the m-scheme reaches 663 527. It is the largest dimension in the present study. We should mention that larger matrix dimensions have been used in other shell-model studies [26], although our calculations include more single-particle states. It should still be feasible to further extend our no-core calculations to higher dimensions than presented here.

In general, good agreement with experiment is found for both the ground-state characteristics as well as the low-lying excited states. We observe underbinding for ^{7}He and ^{7}B. Note that for an isospin invariant interaction these states would be degenerate with the $T = 3/2$ isospin states of ^{7}Li or ^{7}Be. So this underbinding is equivalent to too much spread in the excitation spectrum. This is a common feature in the no-core shell-model calculations, which diminishes as the model-space size increases. Note in Figs. 2 and 3 the correct ordering of excited states in most cases. Also the magnetic moment of ^{7}Li is nicely reproduced. The radii and the quadrupole moments are typically smaller in absolute value in our calculations. We used bare nucleon charges, so there is still need for E2 effective charges despite our large model-space size. By examining the calculated quadrupole matrix elements, we can deduce that effective charges of $e^{\rm p}_{\rm eff} = 1.18e$ and $e^{\rm n}_{\rm eff} = 0.18e$ are needed to obtain the experimental quadrupole moment of ^{7}Li. We note that these effective charges are significantly smaller than the standard effective charges, $e^{\rm p}_{\rm eff} = 1.5e$ and $e^{\rm n}_{\rm eff} = 0.5e$, typically employed in $0\hbar\Omega$ shell-model calculations.

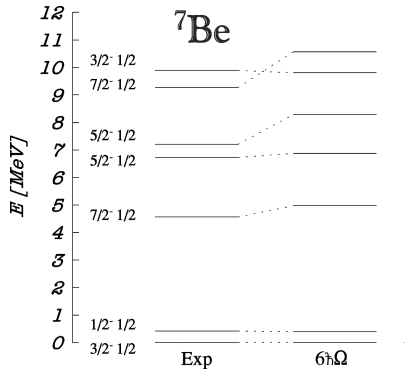

FIG. 3. The experimental and calculated excitation spectra of ^{7}Be. The results corresponding to the model-space size of $6\hbar\Omega$ relative to the unperturbed ground-state configuration are presented. A harmonic-oscillator energy of $\hbar\Omega = 17$ MeV was used.

The ^{7}Li calculation can be compared to the previously published $4\hbar\Omega$ no-core calculation of Ref. [8]. Apart from the larger model-space size in the present calculation, we also take into account more realistically the isospin breaking and derive the effective interaction in a different way. The results are not dramatically different. However, the present $6\hbar\Omega$ calculation provides a better overall agreement with the experiment.

Our results can also be compared to the recent Green's-function Monte Carlo (GFMC) and variational Monte Carlo (VMC) calculations [27]. It should be noted that the GFMC calculations are qualitatively different. No effective interaction is used and the aim is to obtain the exact many-body solutions. As the VMC is an upper bound variational calculation, it is more appropriate to compare the present shell-

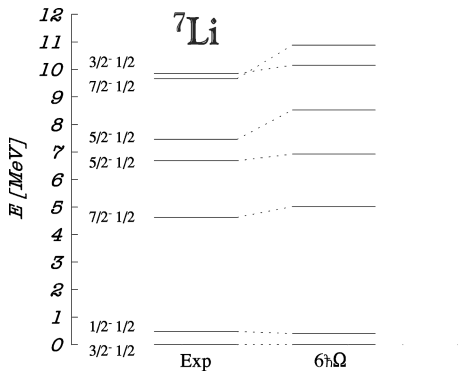

FIG. 2. The experimental and calculated excitation spectra of ^{7}Li. The results corresponding to the model-space size of $6\hbar\Omega$ relative to the unperturbed ground-state configuration are presented. A harmonic-oscillator energy of $\hbar\Omega = 17$ MeV was used.

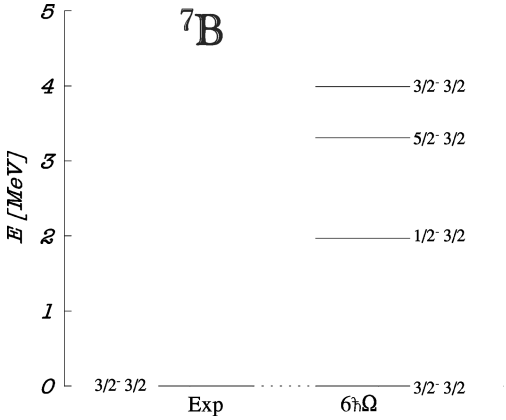

FIG. 4. The experimental and calculated excitation spectra of ^{7}B. The results corresponding to the model-space size of $6\hbar\Omega$ relative to the unperturbed ground-state configuration are presented. A harmonic-oscillator energy of $\hbar\Omega = 17$ MeV was used.

TABLE I. Experimental and calculated ground-state spins and parities; binding energies, in MeV; magnetic moments, in μ_N; quadrupole moments, in e fm^2; and the point proton rms radii, in fm, of the nuclei studied. The results correspond to the $6\hbar\Omega$ for $A=7$ and $4\hbar\Omega$ for $A\geq 8$ calculations, respectively. The harmonic-oscillator parameter was taken to be $\hbar\Omega=17$ MeV for $A=7$ and 8, 16 MeV for $A=9$, 15.5 MeV for $A=10$, and 15 MeV for $A=11$, respectively. The effective interaction used was derived from the Reid93 nucleon-nucleon potential. The Coulomb interaction and isospin breaking in $T=1$ partial waves was taken into account. The same effective interaction was used for all nuclei of a given isobaric chain characterized by A. Bare nucleon charges were used in the calculations. The experimental values are taken from Refs. [28–32].

Isotope	^{7}He		^{7}Li		^{7}Be		^{7}B	
$A=7$	Calc.	Expt.	Calc.	Expt.	Calc.	Expt.	Calc.	Expt.
$J^\pi T$	$\frac{3}{2}^-\frac{3}{2}$	$(\frac{3}{2})^-\frac{3}{2}$	$\frac{3}{2}^-\frac{1}{2}$	$\frac{3}{2}^-\frac{1}{2}$	$\frac{3}{2}^-\frac{1}{2}$	$\frac{3}{2}^-\frac{1}{2}$	$\frac{3}{2}^-\frac{3}{2}$	$(\frac{3}{2})^-\frac{3}{2}$
E_B	26.926	28.82(3)	39.270	39.245	37.632	37.600	22.466	24.72
μ	−1.166		+2.994	+3.256	−1.132		+2.921	
Q	+0.471		−2.710	−4.00(6)	−4.631		+4.338	
$\sqrt{\langle r_p^2\rangle}$	1.692		2.045	2.27(2)	2.216	2.36(2)	2.472	

Isotope	^{8}He		^{8}Li		^{8}Be		^{8}B	
$A=8$	Calc.	Expt.	Calc.	Expt.	Calc.	Expt.	Calc.	Expt.
$J^\pi T$	0^+2	0^+2	2^+1	2^+1	0^+0	0^+0	2^+1	2^+1
E_B	25.426	31.408	36.859	41.277	52.486	56.500	33.033	37.738
μ			+1.419	+1.654			+1.240	1.036
Q			+2.208	+3.11(5)			+4.000	(+)6.83(21)
$\sqrt{\langle r_p^2\rangle}$	1.684	1.76(3)	1.941	2.26(2)	2.071		2.188	2.45(5)

Isotope	^{9}He		^{9}Li		^{9}Be		^{9}B		^{9}C	
$A=9$	Calc.	Expt.	Calc.	Expt.	Calc.	Expt.	Calc.	Expt.	Calc.	Expt.
$J^\pi T$	$\frac{1}{2}^-\frac{5}{2}$	?	$\frac{3}{2}^-\frac{3}{2}$	$\frac{3}{2}^-\frac{3}{2}$	$\frac{3}{2}^-\frac{1}{2}$	$\frac{3}{2}^-\frac{1}{2}$	$\frac{3}{2}^-\frac{1}{2}$	$\frac{3}{2}^-\frac{1}{2}$	$\frac{3}{2}^-\frac{3}{2}$	$(\frac{3}{2}^-)\frac{3}{2}$
E_B	23.048	30.26(6)	40.827	45.341	55.194	58.165	53.082	56.314	34.343	39.034
μ	+0.656		+2.940	3.439	−1.066	−1.178	+2.865		−0.981	1.391
Q			−2.085	−2.74(10)	+3.245	+5.29(4)	+2.582		−2.591	
$\sqrt{\langle r_p^2\rangle}$	1.740		1.946	2.18(2)	2.063	2.34(1)	2.169		2.259	2.48(3)

Isotope	^{10}He		^{10}Li		^{10}Be		^{10}B		^{10}C	
$A=10$	Calc.	Expt.	Calc.	Expt.	Calc.	Expt.	Calc.	Expt.	Calc.	Expt.
$J^\pi T$	0^+2	?	2^+2	? 2	0^+1	0^+1	3^+0	3^+0	0^+1	0^+1
E_B	22.653	30.34(7)	40.923	45.316	63.024	64.977	62.607	64.751	58.194	60.321
μ			+3.105				+1.850	+1.801		
Q			−2.046				+5.643	+8.472		
$\sqrt{\langle r_p^2\rangle}$	1.786		1.958		2.051	2.24(8)	2.127	2.30(12)	2.214	2.31(3)

Isotope	^{11}Li		^{11}Be	
$A=11$	Calc.	Expt.	Calc.	Expt.
$J^\pi T$	$\frac{3}{2}^-\frac{5}{2}$	$\frac{3}{2}^-\frac{5}{2}$	$\frac{1}{2}^-\frac{3}{2}$	$\frac{1}{2}^-\frac{3}{2}$
E_B	43.686	45.64(3)	65.124	65.481
μ	+3.601	3.668	+0.802	
Q	−2.301	−3.12(45)		
$\sqrt{\langle r_p^2\rangle}$	1.986	2.88(11)	2.061	

model calculations with the GFMC, which includes all the statistically sampled correlations in the system. Because the GFMC calculations are much more involved than VMC, they have not been carried out for all excited states. We should also mention that the GFMC and VMC calculations were done with the Argonne V18 interaction. As both the Argonne V18 interaction and the Reid93 interaction (that we used) describe the NN scattering data more-or-less equally well, a different choice of potential should not cause significant difference in the obtained results. In addition, a real three-body interaction was included in the GFMC and VMC, unlike in our calculations. Still, it is interesting to note some similarities between our shell-model calculations and the VMC and GFMC results for $A=7$. Our ^{7}Li calculation shows correct

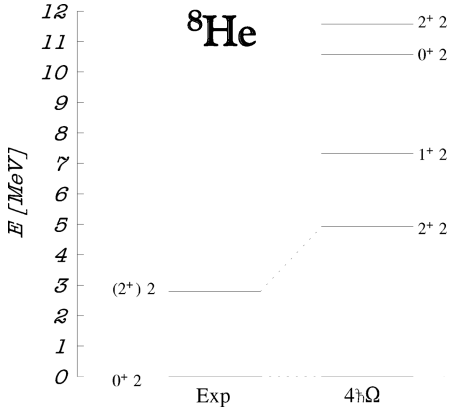

FIG. 5. The experimental and calculated excitation spectra of ^{8}He. The results corresponding to the model-space size of $4\hbar\Omega$ relative to the unperturbed ground-state configuration are presented. A harmonic-oscillator energy of $\hbar\Omega = 17$ MeV was used.

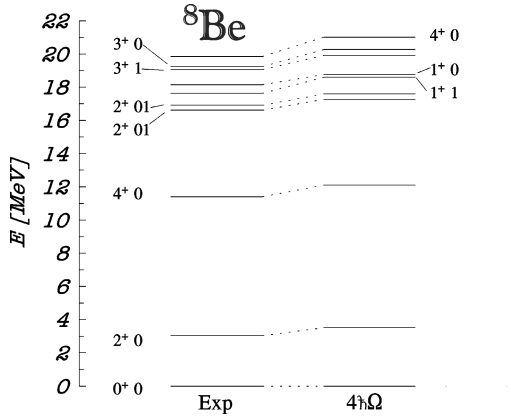

FIG. 7. The experimental and calculated excitation spectra of ^{8}Be. The results corresponding to the model-space size of $4\hbar\Omega$ relative to the unperturbed ground-state configuration are presented. A harmonic-oscillator energy of $\hbar\Omega = 17$ MeV was used.

level ordering for the lowest five states, while the sixth and seventh states are interchanged in comparison to the experiment. The same feature is found in the VMC calculation. Also our higher excited states have energies typically too large, similar to the VMC and GFMC. On the other hand, the excitation spectrum of ^{7}He, obtained in our calculation, has energies about two times higher than those of the VMC, although the level ordering is the same. In addition, in both approaches a larger decrease in the calculated binding energies is observed for isobars with higher ground-state isospin than is observed experimentally.

B. $A = 8$ nuclei

In Figs. 5, 6, 7, and 8 we present the experimental and calculated excitation spectra of ^{8}He, ^{8}Li, ^{8}Be, and ^{8}B, respectively. Their ground-state properties are summarized in Table I. The calculations were performed in a model space of up to $4\hbar\Omega$ excitations relative to the unperturbed ground-state configuration. A harmonic-oscillator frequency of $\hbar\Omega = 17$ MeV was used. As explained earlier in this section, the two-body effective interaction was evaluated using $N_{\max} = 8$. We note that the same effective interaction was used for all the $A = 8$ isobars.

Like in the case of the $A = 7$ nuclei, we obtain a good description of the ground state properties as well as of the low-lying excitation spectra. In particular, for ^{8}Be we have excellent agreement with the experiment for all positive-parity states below the excitation energy of 20 MeV. We note that the $T = 0,1$, $J = 2^+, 1^+, 3^+$ doublets show significant isospin mixing compared to other calculated states. In our calculations, the lower state always has the $T = 1$ component dominant. We note that electromagnetic properties of the 16.6 and 16.9 MeV 2^+ doublet in ^{8}Be were recently analyzed [33]. The doublet has almost equal admixtures of $T = 0$ and $T = 1$ components. In Table II we compare the experimentally extracted isoscalar and isovector electromagnetic transition rates from the doublet with those obtained in our shell-model calculation. Our results can also be compared with other shell-model calculations as presented in Table III of Ref. [33]. In those calculations, phenomenological effective interactions of Refs. [13–15] were employed. Our calculation provides excellent agreement with experiment for the M1 properties and, unlike the other shell-model calculations used for the analysis, gives the positive sign of the isoscalar-isovector matrix element ratio in agreement with experiment. Also, unlike the other shell-model calcula-

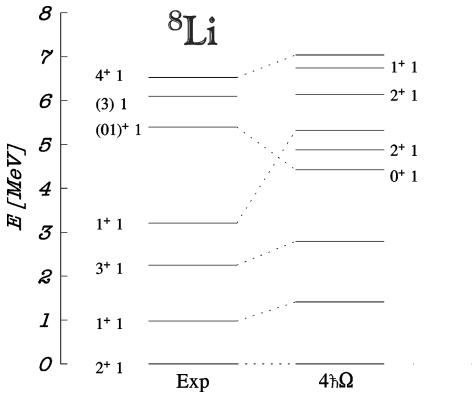

FIG. 6. The experimental and calculated excitation spectra of ^{8}Li. The results corresponding to the model-space size of $4\hbar\Omega$ relative to the unperturbed ground-state configuration are presented. A harmonic-oscillator energy of $\hbar\Omega = 17$ MeV was used.

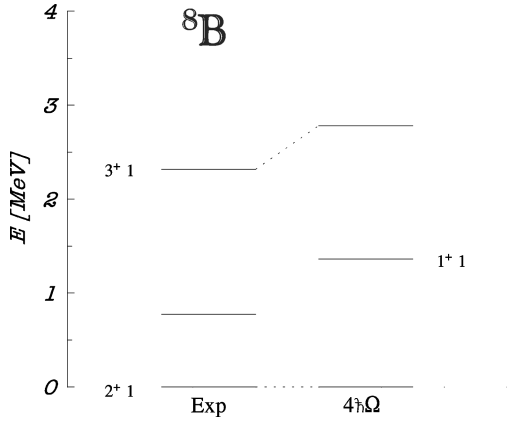

FIG. 8. The experimental and calculated excitation spectra of ^{8}B. The results corresponding to the model-space size of $4\hbar\Omega$ relative to the unperturbed ground-state configuration are presented. A harmonic-oscillator energy of $\hbar\Omega = 17$ MeV was used.

TABLE II. Experimental and calculated properties of transitions from the 16 MeV 2^+ doublet in ^{8}Be. Reduced transition strengths are given in $e^2\text{fm}^4$ for E2 and in μ_N^2 for M1. The observable ϵ is defined as a ratio of the isoscalar and the isovector M1 matrix elements. The mixing ratios δ_0 (δ_1) are computed using the E2 isoscalar (isovector) matrix element and the isovector M1 matrix element. Bare nucleon charges were used in the calculations. The experimental values are taken from Ref. [33].

Final state	Observable	Calc.	Expt.
2^+(3.0 MeV)	B(M1, *IV*)	0.086	0.091 ± 0.006
2^+(3.0 MeV)	B(M1, *IS*)	3×10^{-4}	$(2\pm2)\times10^{-4}$
2^+(3.0 MeV)	ϵ	$+0.057$	$+0.06\pm0.02$
2^+(3.0 MeV)	B(GT)	0.018	0.031
2^+(3.0 MeV)	B(E2, *IV*)	2×10^{-4}	$(1\pm6)\times10^{-3}$
2^+(3.0 MeV)	B(E2, *IS*)	0.063	0.30 ± 0.12
0^+(0.0 MeV)	B(E2, *IV*)	0.024	0.00 ± 0.03 or 0.14 ± 0.03
0^+(0.0 MeV)	B(E2, *IS*)	0.028	0.14 ± 0.03 or 0.00 ± 0.03
2^+(3.0 MeV)	δ_1	$+0.005$	$+0.01\pm0.03$
2^+(3.0 MeV)	δ_0	$+0.099$	$+0.22\pm0.04$

tions discussed, we obtained stronger isoscalar than isovector transition strength for the transition to the $0+$ state. We note that bare nucleon charges were employed in our calculations and that the E2 transitions as well as the quadrupole moments are typically underestimated. This indicates a need for effective E2 charges despite the large model space used. In order to reproduce the ^{8}Li and ^{8}B quadrupole moments, we need average effective charges of $e^p_{\text{eff}}=1.3e$ and $e^n_{\text{eff}}=0.3e$ for this isobaric chain, with smaller values for ^{8}Li than for ^{8}B.

Some excited states of the $A=8$ nuclei have also been calculated using the VMC approach [27]. Our calculation gives similar results for the lowest 2^+0 and 4^+0 states of ^{8}Be. On the other hand, we get higher excitation energies for the 1^+1 and 3^+1 states of ^{8}Li, and in particular for the 4^+1 state of ^{8}Li as well as all the excited states of ^{8}He. The largest difference between our results and the VMC results is in the position of 0^+ states of ^{8}He and ^{8}Li. In the VMC calculations their excitation energy is significantly lower than that obtained in the shell-model calculations. As the VMC gives an upper bound, the GFMC result would be lower still. The ^{8}He nucleus is a weakly bound system, where scattering to the continuum will play an important role in the structure of higher-lying states. Because the harmonic-oscillator basis employed in our shell-model calculations has incorrect asymptotics for the single-particle wave-functions, we would not expect our calculation to describe well the higher-lying states in weakly bound systems.

The magnetic moments obtained in our shell-model calculations for the $A=7$ and $A=8$ nuclei are in some cases in a better agreement with the experiment than those obtained by the VMC. On the other hand, we obtain smaller quadrupole moments compared to both the experiment and the VMC. Also the rms proton radii are about 10% smaller than those obtained in the VMC calculations.

C. $A=9$ nuclei

The experimental and calculated negative-parity excitation spectra of the ^{9}He, ^{9}Li, ^{9}Be, ^{9}B, and ^{9}C nuclei are presented in Figs. 9, 10, 11, 12, and 13, respectively. Their ground state properties are shown in Table I. The calculations were performed in the $4\hbar\Omega$ relative to the unperturbed ground-state configuration model space. We used a harmonic-oscillator frequency of $\hbar\Omega=16$ MeV. As for all

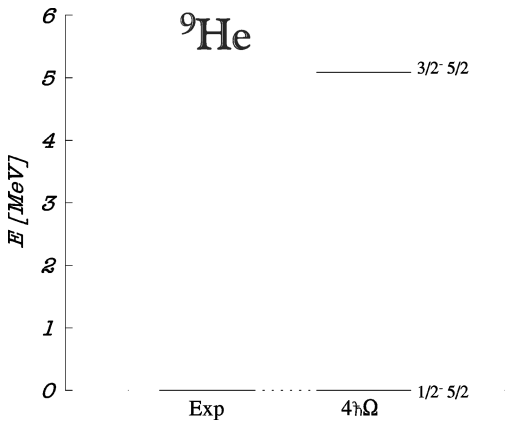

FIG. 9. The experimental and calculated excitation spectra of ^{9}He. The results corresponding to the model-space size of $4\hbar\Omega$ relative to the unperturbed ground-state configuration are presented. A harmonic-oscillator energy of $\hbar\Omega=16$ MeV was used.

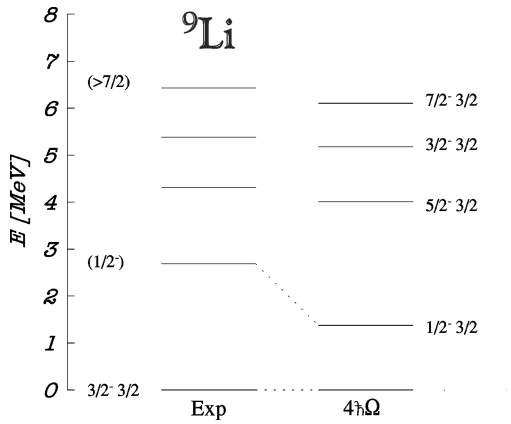

FIG. 10. The experimental and calculated excitation spectra of ^{9}Li. The results corresponding to the model-space size of $4\hbar\Omega$ relative to the unperturbed ground-state configuration are presented. A harmonic-oscillator energy of $\hbar\Omega=16$ MeV was used.

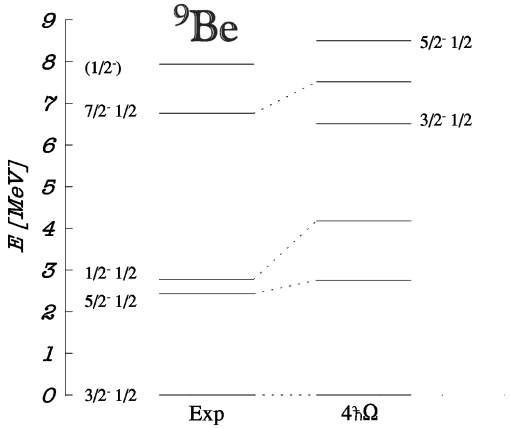

FIG. 11. The experimental and calculated excitation spectra of ^{9}Be. The results corresponding to the model-space size of $4\hbar\Omega$ relative to the unperturbed ground-state configuration are presented. A harmonic-oscillator energy of $\hbar\Omega = 16$ MeV was used.

the nuclei with $A \geqslant 8$, the two-body effective interaction was evaluated using $N_{\max} = 8$ with no additional free parameter. The same effective interaction was employed for all the $A = 9$ nuclei.

There are few experimental data available, in particular for the ^{9}He, ^{9}Li, and ^{9}C nuclides. In addition, there are no GFMC or VMC calculations, with which we can make a comparison. In general, we obtain a correct level ordering for the lowest states. Also the known magnetic moments are reasonably reproduced. As in the case of other isobaric chains, the calculated absolute values of the quadrupole moments are smaller than the experimental ones. To reproduce the ^{9}Li and ^{9}Be quadrupole moments, we would need average effective charges of $e^{\mathrm{p}}_{\mathrm{eff}} = 1.25e$ and $e^{\mathrm{n}}_{\mathrm{eff}} = 0.25e$ for this isobaric chain, with smaller values for ^{9}Li than for ^{9}Be.

Our predictions for the experimentally unknown magnetic moments, quadrupole moments, and point-proton rms radii for ^{9}He, ^{9}B, and ^{9}C are given in Table I.

D. $A = 10$ nuclei

We performed extensive calculations for $A = 10$ nuclei in order to evaluate the isospin-mixing correction of the ^{10}C

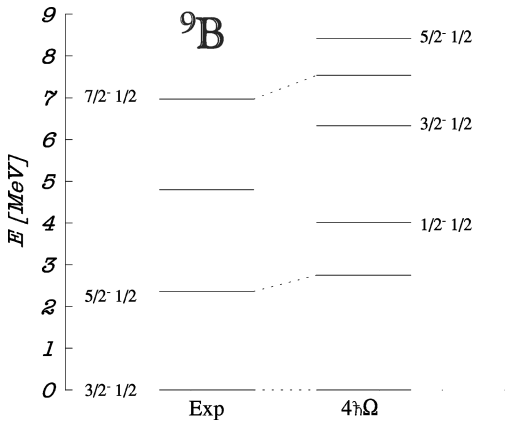

FIG. 12. The experimental and calculated excitation spectra of ^{9}B. The results corresponding to the model-space size of $4\hbar\Omega$ relative to the unperturbed ground-state configuration are presented. A harmonic-oscillator energy of $\hbar\Omega = 16$ MeV was used.

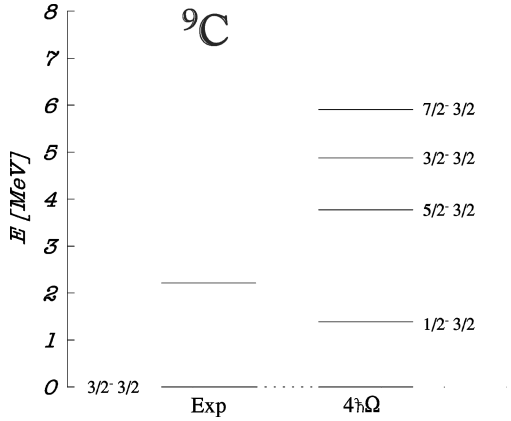

FIG. 13. The experimental and calculated excitation spectra of ^{9}C. The results corresponding to the model-space size of $4\hbar\Omega$ relative to the unperturbed ground-state configuration are presented. A harmonic-oscillator energy of $\hbar\Omega = 16$ MeV was used.

$\rightarrow$ ^{10}B Fermi transition. Those calculations were published in Ref. [11]. Here we complement the published results with the calculation for ^{10}He and ^{10}Li. We used the same effective interactions as in Ref. [11]. The calculations were performed in the $4\hbar\Omega$ model space. In Fig. 14 we present the dependence of the ^{10}Li spectra on the harmonic-oscillator frequency for $\hbar\Omega = 14$, 15.5, and 17 MeV. Despite the recent new measurements of ^{10}Li properties [34], a controversy on the spin-parity assignment of the ground state of this nucleus remains. Our calculation prefers 2^+2 as the lowest positive-parity state for all the choices of $\hbar\Omega$. For $\hbar\Omega = 14$ MeV, the $1^+, 2^+$ doublet becomes almost degenerate, however. We should note that, as discussed above for the ^{8}He calculation, the shell-model single-particle wave-functions have incorrect asymptotics. The shell-model approach is, therefore, not quite suitable for the description of weakly bound states or resonances. A similar dependence on $\hbar\Omega$ for ^{10}B was studied in Ref. [11]. There we found a sensitivity of the ground state to $\hbar\Omega$. Only for $\hbar\Omega = 17$ MeV did we obtain the correct ground-state spin 3^+0, while for $\hbar\Omega = 14$ and 15.5 MeV the calculated ground state was 1^+0. In Fig. 15 we present

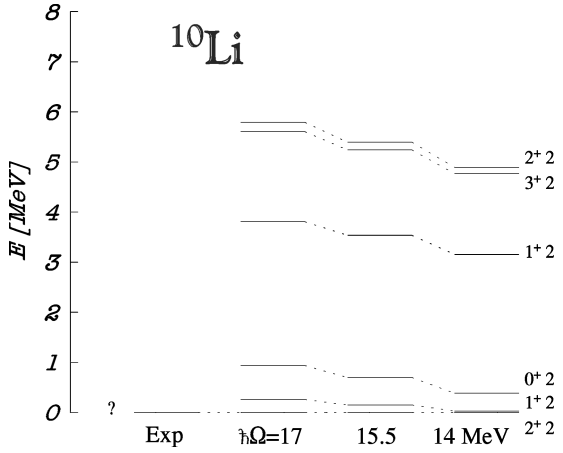

FIG. 14. The dependence of the spectra of ^{10}Li on the harmonic-oscillator energy for $\hbar\Omega = 14$ MeV, 15.5 MeV, and 17 MeV, respectively. The results corresponding to the model-space size of $4\hbar\Omega$ relative to the unperturbed ground-state configuration are presented.

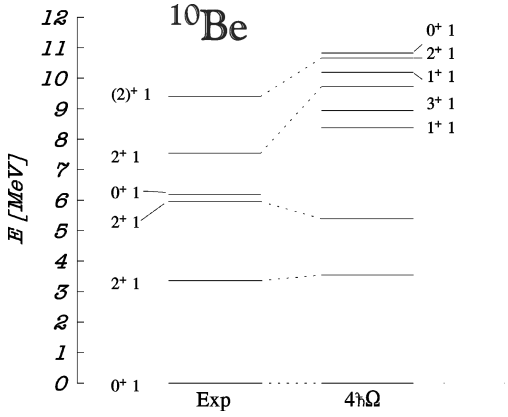

FIG. 15. The experimental and calculated excitation spectra of ^{10}Be. The results corresponding to the model-space size of $4\hbar\Omega$ relative to the unperturbed ground-state configuration are presented. A harmonic-oscillator energy of $\hbar\Omega = 15.5$ MeV was used.

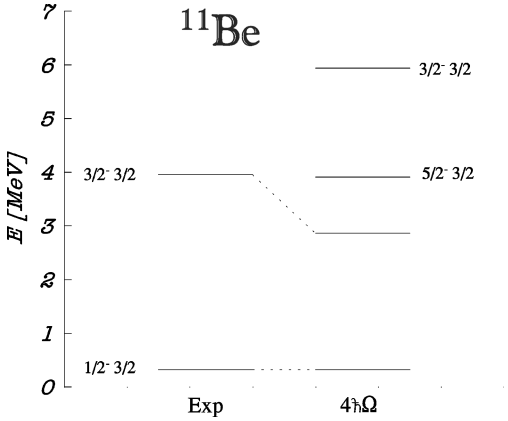

FIG. 16. The experimental and calculated excitation spectra of ^{11}Be. The results corresponding to the model-space size of $4\hbar\Omega$ relative to the unperturbed negative-parity ground-state configuration are presented. A harmonic-oscillator energy of $\hbar\Omega = 15$ MeV was used. Note that the ground state of this nucleus has positive parity. The energy of the calculated $\frac{1}{2}^-$ state is set equal to the lowest experimental negative-parity state.

the spectrum of ^{10}Be obtained in the $4\hbar\Omega$ model space with $\hbar\Omega = 15.5$ MeV. As discussed in Ref. [11], the excited 0^+1 state, assumed to be dominated by a $2\hbar\Omega$ configuration, is not obtained below 10 MeV in our calculation. It is likely that our $4\hbar\Omega$ model space is not large enough to give the right description of such a state.

In Table I, we present the experimental and calculated ground-state properties of the $A = 10$ nuclei. Part of the results overlap with those presented in Table I of Ref. [11]. As explained above, the calculated ^{10}B 3^+0 for $\hbar\Omega = 15.5$ MeV is the first-excited state, lying 0.17 MeV above the 1^+0. This is the only case in our study, where the incorrect ground-state spin is obtained. The right level ordering is recovered for this nucleus, however, when $\hbar\Omega$ is increased to, e.g., 17 MeV. The results presented in Table I were evaluated using bare nucleon charges. In order to reproduce the ^{10}B experimental quadrupole moment, we need effective charges of $e^{\rm p}_{\rm eff} = 1.25e$ and $e^{\rm n}_{\rm eff} = 0.25e$.

From the binding energy results given in Table I, we can deduce the energy splitting between isospin-analog states. In most cases our calculated splitting is larger than the corresponding experimental splitting, though the difference does not exceed about 10%. Mainly the Coulomb energy is responsible for the isospin-analog-state splitting. As our calculated proton radii are typically smaller than the experimental ones, we obtain stronger Coulomb splitting. We discussed this point in Ref. [11] and pointed out the importance of the correct value of the proton radius in order to get the correct isospin-analog-state splitting.

E. $A = 11$ nuclei

For $A = 11$ nuclei we performed calculations only for the ^{11}Li and ^{11}Be. In the last part of Table I we show the ground-state properties of ^{11}Li and the lowest negative-parity state of ^{11}Be. In Fig. 16 we present the experimental and calculated negative-parity spectra of ^{11}Be. The calculations were performed in the $4\hbar\Omega$ model space using $\hbar\Omega = 15$ MeV.

We note that the ground state of ^{11}Be is a positive-parity state $\frac{1}{2}^+$. We also performed calculations for the positive parity states in the $3\hbar\Omega$ model space. We got a correct level ordering for the lowest positive-parity states. However, those states were shifted with respect to the negative-parity states by 5.56 MeV, so that the calculated ground state has a negative parity. It should be realized that the relative position of the positive- and negative-parity states depends on the size of the respective model spaces. It is quite likely that a $5\hbar\Omega$ model-space calculation would result in a positive-parity ground state.

Our $4\hbar\Omega$ model space is insufficient for reproducing the halo properties of the ^{11}Li nucleus. This is seen, in particular, in a smaller calculated point-proton rms radius as well as a smaller absolute value of the quadrupole moment compared with the experiment. In order to reproduce the ^{11}Li experimental quadrupole moment, we need effective charges of $e^{\rm p}_{\rm eff} = 1.27e$ and $e^{\rm n}_{\rm eff} = 0.27e$. On the other hand, we easily obtain the correct ground-state spin, a reasonable binding energy, as well as the magnetic moment.

We note that the rms point-proton radii obtained in our calculations are smaller than the experimental ones with the largest discrepancies for ^{8,9,11}Li and ^{8}B, e.g., nuclei far from the stability. One should remark, however, that the experimental extraction of the rms radii is model dependent.

IV. CONCLUSIONS

We have performed large-basis no-core shell-model calculations for selected $0p$-shell nuclei with $A = 7 - 11$. We used two-body effective interactions derived from the Reid93 nucleon-nucleon potential with the isospin breaking taken into account. We were able to reproduce most of the characteristics of the ground states as well as the correct ordering of the lowest excited states. As discussed in detail in Sec. III, our no-core shell-model approach has only a very limited number of freely adjustable parameters, such as the harmonic-oscillator frequency and the size of the model space. The calculations were performed in the $6\hbar\Omega$ and $4\hbar\Omega$ model spaces for the $A = 7$ and $A = 8 - 11$ nuclei, respectively. Our results show that the multiconfiguration shell-model approach combined with the use of microscopic

effective interactions, is capable of a good qualitative and quantitative description of the $0p$-shell nuclei.

It is feasible to extend the present $4\hbar\Omega$ calculations to heavier $0p$-shell nuclei as well. For those nuclei, slightly higher m-scheme dimensions than in the present calculations will have to be dealt with. The present results can be used for calculating electromagnetic and weak properties and scattering characteristics as well as other applications, such as, e.g., $^7\mathrm{Be}+p\leftrightarrow{}^8\mathrm{B}$ nuclear vertex constant. With regard to the effective-interaction theory, it is desirable to eliminate some of the free parameters still present in the calculations by using three-body effective interactions. In particular, we should be able to eliminate the treatment of the two-nucleon model-space size parameter $N_{\max}$ as an adjustable parameter, or alternatively the use of the parameter k_Q employed in our $6\hbar\Omega$ calculations, in this way. Also, the use of the three-body effective interaction should weaken the dependence on the harmonic-oscillator frequency. We are presently investigating this aspect in four-nucleon shell-model calculations. A complete elimination of the dependence of the results on the harmonic-oscillator frequency will hardly be achieved, however, in the model-spaces of only a few $\hbar\Omega$ above the unperturbed ground-state configuration, although it can be greatly weakened. Our investigation of the three-nucleon shell-model calculations [25] supports this statement. Most likely, the three-body effective interaction should not be used directly as an input into the shell-model calculation, but rather it should be utilized for renormalizing the two-body effective interactions. Work in this direction is underway.

ACKNOWLEDGMENTS

We thank R. Wiringa for useful comments. One of us (B.R.B.) would like to thank Hans Weidenmüller and the Max-Planck-Institut für Kernphysik, Heidelberg, and Peter von Brentano and the Institut für Kernphysik, Köln, Germany, for their hospitality and partial support during the latter stages of this work. This work was supported by the NSF Grant No. PHY96-05192. P.N. also acknowledges partial support from the grant of the Grant Agency of the Czech Republic 202/96/1562.

[1] D. C. Zheng, B. R. Barrett, L. Jaqua, J. P. Vary, and R. J. McCarthy, Phys. Rev. C **48**, 1083 (1993).
[2] L. Jaqua, D. C. Zheng, B. R. Barrett, and J. P. Vary, Phys. Rev. C **48**, 1765 (1993).
[3] L. Jaqua, P. Halse, B. R. Barrett, and J. P. Vary, Nucl. Phys. **A571**, 242 (1994).
[4] D. C. Zheng, B. R. Barrett, J. P. Vary, and R. J. McCarthy, Phys. Rev. C **49**, 1999 (1994).
[5] D. C. Zheng and B. R. Barrett, Phys. Rev. C **49**, 3342 (1994).
[6] D. C. Zheng, J. P. Vary, and B. R. Barrett, Phys. Rev. C **50**, 2841 (1994).
[7] D. C. Zheng, B. R. Barrett, J. P. Vary, and H. Müther, Phys. Rev. C **51**, 2471 (1995).
[8] D. C. Zheng, B. R. Barrett, J. P. Vary, W. C. Haxton, and C. L. Song, Phys. Rev. C **52**, 2488 (1995).
[9] P. Navrátil and B. R. Barrett, Phys. Rev. C **54**, 2986 (1996).
[10] P. Navrátil, M. Thoresen, and B. R. Barrett, Phys. Rev. C **55**, R573 (1997).
[11] P. Navrátil, B. R. Barrett, and W. E. Ormand, Phys. Rev. C **56**, 2542 (1997).
[12] S. Karataglidis, B. A. Brown, K. Amos, and P. J. Dortmans, Phys. Rev. C **55**, 2826 (1997).
[13] S. Cohen and D. Kurath, Nucl. Phys. **73**, 1 (1965).
[14] N. Kumar, Nucl. Phys. **A225**, 221 (1974).
[15] A. G. M. van Hees, A. A. Wolters, and P. W. M. Glaudemans, Nucl. Phys. **A476**, 61 (1988).
[16] E. K. Warburton and B. A. Brown, Phys. Rev. C **46**, 923 (1992).
[17] N. A. F. M. Poppelier, A. A. Wolters, and P. W. M. Glaudemans, Z. Phys. A **346**, 11 (1993).
[18] K. Suzuki and S. Y. Lee, Prog. Theor. Phys. **64**, 2091 (1980).
[19] K. Suzuki, Prog. Theor. Phys. **68**, 246 (1982); K. Suzuki and R. Okamoto, *ibid.* **70**, 439 (1983).
[20] P. Navrátil and B. R. Barrett, Phys. Lett. B **369**, 193 (1996).
[21] V. G. J. Stoks, R. A. M. Klomp, C. P. F. Terheggen, and J. J. de Swart, Phys. Rev. C **49**, 2950 (1994).
[22] J. P. Vary and D. C. Zheng (unpublished).
[23] B. R. Barrett, R. G. L. Hewitt, and R. J. McCarthy, Phys. Rev. C **3**, 1137 (1971).
[24] M. Hjorth-Jensen, T. T. S. Kuo, and E. Osnes, Phys. Rep. **261**, 125 (1995).
[25] P. Navrátil and B. R. Barrett, Phys. Rev. C **57**, 562 (1998).
[26] E. Caurier, F. Nowacki, A. Poves, and J. Retamosa, Phys. Rev. Lett. **77**, 1954 (1996).
[27] B. S. Pudliner, V. R. Pandharipande, J. Carlson, S. C. Pieper, and R. B. Wiringa, Phys. Rev. C **56**, 1720 (1997); R. B. Wiringa, Argonne National Laboratory preprint PHY-8806-TH-97, Proceedings of XV Few-Body Conference [Nucl. Phys. A (to be published)].
[28] F. Ajzenberg-Selove, Nucl. Phys. **A490**, 1 (1988).
[29] H. De Vries, C. W. Dejager, and C. De Vries, At. Data Nucl. Data Tables **36**, 495 (1987).
[30] I. Tanihata, T. Kobayashi, O. Yamakawa, S. Shimoura, K. Ekuni, K. Sugimoto, N. Takahashi, T. Shimoda, and H. Sato, Phys. Lett. B **206**, 592 (1988).
[31] I. Tanihata, D. Hirata, T. Kobayashi, S. Shimoura, K. Sugimoto, and H. Toki, Phys. Lett. B **289**, 261 (1992).
[32] A. Ozawa, I. Tanihata, T. Kobayashi, Y. Sugahara, O. Yamakawa, K. Omata, K. Sugimoto, D. Olson, W. Christie, and H. Wieman, Nucl. Phys. **A608**, 63 (1996).
[33] L. De Braeckeleer *et al.*, Phys. Rev. C **51**, 2778 (1995).
[34] H. G. Bohlen, W. von Oertzen, Th. Stolla, R. Kalpakchieva, B. Gebauer, M. Wilpert, Th. Wilpert, A. N. Ostrowski, S. M. Grimes, and T. N. Massey, Nucl. Phys. **A616**, 254c (1997); M. Zinser *et al.*, *ibid.* **A619**, 151 (1997).